Title
REPORT ON TOF AT 900 MeV/nuc Au IONS

Author
Crawford, H.J.

Publication Date
1985-10-01

LBL-20372
Preprint

Lawrence Berkeley Laboratory
UNIVERSITY OF CALIFORNIA

Submitted to Nuclear Instruments and Methods

REPORT ON TOF AT 900 MeV/nuc Au IONS

H.J. Crawford, I. Flores, P.J. Lindstrom,
and G. Krebs

October 1985

NUCLEAR SCIENCE DIVISION

Prepared for the U.S. Department of Energy under Contract DE-AC03-76SF00098

DISCLAIMER

LBL-20372

Report on TOF for 900 MeV/nuc Au Ions

H.J. Crawford and I. Flores

Space Sciences Laboratory
University of California
Berkeley, CA 94720

P.J. Lindstrom and G. Krebs

Nuclear Science Division
Lawrence Berkeley Laboratory
University of California
Berkeley, CA 94720

*This work was supported in part by the Director, Office of Energy Research, Division of Nuclear Physics of the Office of High Energy and Nuclear Physics of the U.S. Department of Energy under Contract No. DE-AC03-76SF00098 and by NASA grant NGR 05-003-513.

Report on TOF for 900 MeV/nuc Au Ions

H.J. Crawford and I. Flores

Space Sciences Laboratory
University of California
Berkeley, CA 94720

P.J. Lindstrom and G. Krebs

Nuclear Science Division
Lawrence Berkeley Laboratory
University of California
Berkeley, CA 94720

1. Introduction

This note describes our measurements of the time-of-flight (TOF) of 900 MeV/nuc Au ions at the Lawrence Berkeley Laboratory Bevalac (ref.1) as part of an investigation of relativistic and higher order (Z^3) terms in the range-energy relation for heavy ions traversing matter (ref.2). The goal of this measurement was to provide beam energies to an accuracy of better than 0.5% at 900 MeV/nuc. Using two small scintillators and a flight path of 18.5*m* we achieved time resolutions of better than 40*ps* per detector and an overall energy resolution of better than 0.4% (3 MeV/nuc). This resolution can be improved using faster tubes and faster scintillator. We discuss in an appendix the variation of energies within a Bevalac "spill".

2. Setup

The setup of the beam line and scintillators is shown in Figure 1. In the "T0" position, scintillator S2 was placed 5cm behind S1 in the same vacuum box. Each scintillator was in a cylindrical, light tight container, having walls in the beam direction of 0.001" Al foil. In the "T1" position, S2 was moved out of the vacuum to a remote controlled cart in the cave area.

*This work was supported in part by the Director, Office of Energy Research, Division of Nuclear Physics of the Office of High Energy and Nuclear Physics of the U.S. Department of Energy under Contract No. DE-AC03-76SF00098 and by NASA grant NGR 05-003-513.

Note that the same scintillator, cables and electronics were used in the T0 and Tl positions. The Tl flight path was vacuum from S1 to within 10cm of S2, the vacuum being sealed with a 0.004″ thick Al window.

a. Distance

The distance between the center of S2 at position T0 and at position T1 was measured using a standard Starrett steel tape which is quoted as having a thermal coefficient of expansion of $4.6 \times 10^{-6}/^{0}Ccm.$ and an overall accuracy at $20°C$ of $\leqslant 0.17cm$ for a 2000 cm distance. We use an uncertainty in this measurement from the tape measure as $0.17cm.$ Errors in the measured flight path due to distortions in particle trajectories caused by quadrupole focussing are less than $0.1cm.$ We measured the distance on separate days and found no systematic variation in the value of $1846.9 \pm 0.1cm.$ We assign a total uncertainty to the distance measurement of $\pm 0.2cm.$ The flight time is then the difference between the TDC value for the T0 and T1 positions.

b. Scintillators

The scintillator material used was Pilot F which has a decay time of $2.5ns.$ (Note that $1.5ns$ scintillator is now available in test quantities and would significantly increase the fast photon yield in the system). S1 was $1.8mm$ thick while S2 was $6mm$ thick. Each scintillator was only $2mm$ wide (perpendicular to the beam) to minimize transit time variations in the scintillator. This contributes $\approx 5ps/mm$ to time spread in situations where track location in the scintillator is unknown. As shown in Fig.1, no light guide was used. The difference in light path from the extremes of the scintillator is $\approx \pm 10ps$, dominated by the difference in position on the face of the scintillator. Transit time for the particle passing through the scintillator is $\approx 3ps/mm$ meaning that energy depositied at the entrance of each scintillator can begin light production a few ps before light production from the exit of the scintillator.

c. Phototube

Each scintillator was viewed by a single Amperex XP2972 photomultiplier tube from a distance of 3.2*cm*. These tubes are specified as having 1.9*ns* risetimes and gains up to 9×10^6. The high voltage divider chain was configured as shown in Fig.2. We do not have a specification of the variation in risetime pulse to pulse expected from this tube.

d. Electronics

The electronics used is diagrammed in Figure 3 and consists primarily of a coincidence and busy circuit. Modules, and channels within modules, were selected to minimize electronic noise. Pulsing at the initial discriminator inputs of Fig.3 resulted in a full-width-at-one-tenth-maximum of less than a single channel (30*ps*) for the electronics alone. Discriminator thresholds were set at 50*mv* for 500*mv* signals. Module types are given in the caption.

e. Pulser

We pulsed the system using an ORTEC model 457 time calibrator. We assume that the pulse period is 20 ± 0.01*ns* as specified by ORTEC through the NBS. This sets the overall time scale for our measurement. This is essential to our measurement of an absolute time interval but irrelevant in most relative time measurements.

f. TDC's

We used 2 LeCroy 2228A type TDCs, one operated in normal fashion at 50*ps/channel* and the second modified to have a sensitivity of 30*ps/channel*. The TDCs were calibrated by triggering the system with the Ortec 457 start pulse and stopping the TDC channels with the Ortec 457 stop pulses. We repeated this calibration many times over the course of setup and running the experiment. The response between channels 200 and 2000 of the

TDCs was uniform and linear so that a channel to time calibration accurate and reproducible to 1/2000 was attained.

g. ADC's

The ADC used was an LRS-2259 peak sensing ADC. We used this in conjunction with a leading edge discriminator because the discriminator is sensitive to the input pulse shape and a peak sensing ADC is more sensitive to pulse shape than a charge integrating ADC. Note that the risetime expected by this ADC is to be at least 50*ns* but our input pulses had rise times of 1.9*ns*. We investigated the effect of this by varying the rise time of an input pulser and showed that the ADC was an excellent measurer of rise time.

h. Data acquisition

The data from this setup was taken through CAMAC using the DATACQ program running an MBD on a DEC 11/45 computer. Online and off-line analysis was performed using the program shell LULU (ref.3). A 50 kHz clock was used to tag the time of each event within a "spill", with the clock reset at the beginning of each spill. This allowed us to investigate energy variations within each spill which may result from the acceleration/extraction process. In addition, each spill was tagged with a "header" event in which the time, "flattop" magnetic field (B) and final accelerating frequency were recorded.

3. Results

We determined the total flight time and hence the particle velocities using our 50*ps/channel* normal TDC. The total flight time was 71*ns*., well within the 100*ns* range of the 50*ps* TDC but outside the 60*ns* of the modified 30*ps* TDC. The 30*ps* TDC was then used to check individual particle resolution and,with an additional delay cable, the "absolute" time.

The T0 TDC spectrum for all 50*ps* data is shown in Fig.4. Note the tails and broad shoulder which can be removed using an ADC cut on both S1 and S2. This effect is illustrated in Fig.5 where we show the TDC vs ADC1 correlation. Placing a tight ADC cut on both S1 and S2 (100 channels wide, 20-50% of the data), we eliminate most of the noise in the TDC spectrum and end up with the TDC distribution shown in Fig.6.

We fit this peak with a Gaussian distribution to obtain the mean value and the standard deviation width σ. Making a final correction for the residual ADC correlation results in a decrease in the per-particle σ but does not alter the mean value. We repeated this T0 measurement three times during the span of 2 hours and reproduced the mean value of 275.7 channels to within 0.03 channels each time.

The TDC spectrum from the T1 position is shown in Fig.7. We fit this to a Gaussian to obtain the mean and σ. For comparison between T0 and T1, exactly the same ADC cuts and TDC/ADC correction function must be used. Again, we repeated the T1 measurement three times for this electronics, reproducing the mean value of 1730.9 to within 0.02 channels. Using consistent cuts on different regions of the ADC spectrum gave identical total transit times to within 0.02 channel.

a. TDC calibration

To convert these channel values to time, we calibrated our TDCs using the NBS-ORTEC time calibrator. This was set to produce time pulses separated by $20.00 +/- 0.01ns$. Assuming this period to be exact, we calibrated both the *"50ps/channel"* and our modified *"30ps/channel"* LeCroy TDCs. Both linearity and differential linearity were checked for these units. The best *"50ps"* channel and the best *"30ps"* channel were chosen and used to record simultaneously the TDC stop signal. This calibration yielded $49.31 \pm 0.02ps/channel$ for our standard TDC.

b. Energy calculation

We calculate the total transit time as

$$(1730.9-275.7)chns \times 49.31ps/chn = 71.756\text{ns} \quad .$$

We calculate β from the distance and time as $\beta = D/cT$. The uncertainty in β is then $d\beta/\beta = ((dD/D)^2 + (dT/T)^2)^{1/2}$. For our measurement this yields

$$\beta = 0.8585 \pm 0.0003$$

which gives an energy leaving the S1 scintillator of 885.1 MeV/nuc.

The uncertainty in this energy from the measurement of time and distance can be calculated as follows. Since $E = \gamma M = (1 - \beta^2)^{-1/2} M$ we find

$$dE/d\beta = \beta\gamma^2 E$$

or

$$dE/E = (\beta\gamma)^2 d\beta/\beta$$

Since $E = K + M$ where K = kinetic energy and M = mass, we find

$$dK/K = ((K + M)(K + 2M)/M^2) \times (d\beta/\beta)$$

which means that $E = 885 \pm 1.8$ MeV/nuc out of scintillator S1.

c. Correction for S1

To obtain the energy of the incident beam, we must correct for the energy loss in the scintillator S1. We did not have time to insert an additional piece identical to S1. However, we measured T0 and T1 both with and without a monitor scintillator S0 in the beam. This scintillator was measured to be 0.238″ thick with a layer of 0.001″ Al and black tape on front and back surfaces. The tape/Al combination was measured to be 0.055 g/cm^2 thick; (0.014 g/cm^2 Al and 0.041 g/cm^2 ″tape″). This combination resulted in a measured energy loss of 50.7 MeV/nuc. We can calculate an energy loss of 2.58

MeV/nuc in the tape, assuming it is all carbon. We can calculate an energy loss of 0.65 MeV/nuc in the Al foils. This leaves an energy loss of 47.5 MeV/nuc in the thick scintillator. Scaling this by the relative thickness of S1, we find an energy loss of 0.070/0.238 × 47.5 = 13.97 MeV/nuc in the S1 scintillator. Adding in the energy loss of the Al foils that covered the windows of the S1 holder we get a total correction of 14.6 MeV/nuc. The correction is limited by our ability to calculate dE/dx in the individual materials and introduces an additional uncertainty in our energy measurement of approximately 2 MeV/nuc.

This gives as our final answer an energy of 899.7 ± 3 MeV/nuc for our Au beam.

4. Discussion

We have been able to make a precise time measurement because of the high light output of relativistic Au ions in scintillator. The ions lose ≈ 2.2 *GeV* in S1 and ≈ 7.7 *GeV* in S2. Assuming it takes ≈ 100*ev* to produce a photon, this leads to 2.2×10^7 photons from S1. The geometry of the S1-PMT arrangement would lead to $\approx$8k photons hitting the photocathode within 25*ps* of the transit of the ion through the scintillator. Known saturation of the scintillator reduces this light output significantly, but there are still hundreds of photons on the photocathode within 25*ps*.

Our measurements can be improved in at least two simple ways. To avoid difficulties with correction for the S1 scintillator, we are arranging to have a duplicate of this scintillator plungable at just upstream of the S1 position. Thus we can measure its effect directly. We also plan to replace the S1 and S2 scintillators with small diffusing surface Cherenkov light sources. This will reduce the total number of photons but all photons will arrive at the photocathode "simultaneously".

Acknowledgments:

We would like to thank Jose Alonso and the Bevalac crew for help in staging and performing this measurement. We thank Steve Durbin at LeCroy Research for help with modification of the TDC, and J.P. Dufour and F. Bieser for help with tube base construction. We also thank H. Yee and P. Conant for help in preparing this manuscript. This work was supported in part by the Director, Office of Energy Research, Division of Nuclear Physics of the Office of High Energy and Nuclear Physics, of the U.S. Department of Energy under Contract DE-AC03-76SF00098 and in part by NASA Grant NGR 05-003-513.

Appendix - energy variation in spill

We included a "clock" value for each event to see if there is any energy variation during the spill. This clock was simply a scaler counting a 50 kHz pulser with the scaler reset at the beginning of "flattop" for each spill. To perform this analysis we used the "30*ps/channel*" TDC to get maximum sensitivity.

First we corrected the TDC for ADC dependence, using a linear function for both ADC1 and ADC2 as seen in Fig.8. The corrected TDC values are plotted against the event clock in Fig.9. We then fit a straight line to this data, yielding a slope of .072*ps/ms*, i.e., a change in transit time of 0.072 ps for each ms after the spill starts. This indicates that, over the course of a 320*ms* spill, the transit time decreases by 23 ps in the mean, with the slower particles coming out of the machine early in the spill. Converting this to a difference in momentum we find that the the particle momentum varies by 10^{-3} over the course of the spill. When we correct our data for this time dependence we find that the remaining time resolution, as shown in Fig.10, is $\sigma = 58\ ps$ per particle.

References

1. Pirruccello, M.C. and C.Tobias, LBL 11220, 1985.

2. S.P.Ahlen, Phys.Rev.A 125, 1856, 1982.
Waddington,C.J.,et al., Phys.Rev.A.,1985.

3. Crawford,H.J. and P.J.Lindstrom, IEEE Transaction in Nuclear Science NS-30, 5, 3842, 1983.

Figure Captions

1. Experimental setup in the Beam 40 line at the Bevalac. Scintillator S1 is $10 \times 2 \times 1.8mm^3$ and S2 is $10 \times 2 \times 6mm^3$. At the "TOF START" position, both scintillators are placed in a vacuum box to get the relative time offset. This is the T0 position. Beam was focused just upstream of the S1 scintillator, with 30% of the full beam hitting S1.

2. Electronics diagram for TOF measurement. Discriminators were LBL MECL III leading edge. TDCs were LeCroy 2228A, one unit modified to have 30*ps/channel* instead of the normal 50*ps/channel*. ADCs were LeCroy 2259A peak sensing.

3. High voltage divider network used in base of XP2972 photomultiplier tubes.

4. T0 distribution for all data. For our energy analysis we used the "50*ps*" TDC, rather than the "30*ps*" TDC as discussed in the text.

5. The ADC - TDC correlation for ADC1. Data used in our analysis were cut on both ADC1 and ADC2 values.

6. T0 distribution after cutting on the ADC values. The $\sigma = 1.4$ implies a 70*ps* per particle resolution.

7. The T1 distribution cut on ADC values.

8. The residual ADC dependence in the "30*ps*" TDC after cutting on ADC1 and ADC2. The slope of the line is -0.003.

9. The TDC correlation with time in the spill. Each "clok" pulse is $20\mu s$. The slope indicates a change of 23*ps* over the 320*ms* spill.

10. Final TDC resolution after removing residual ADC and clock correlations is shown to be $\sigma = 58ps$.

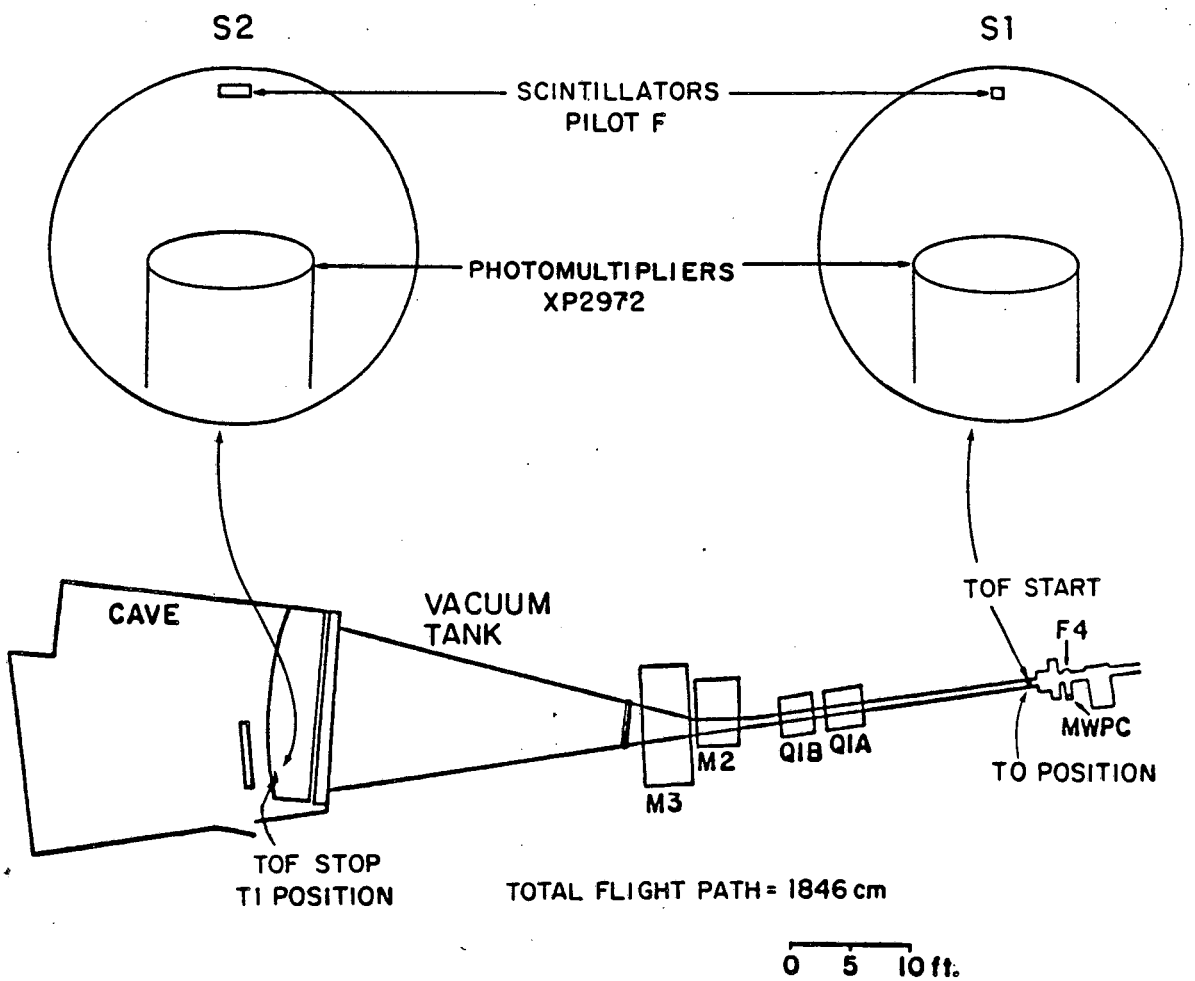

FIG. 1

XBL 859-3994

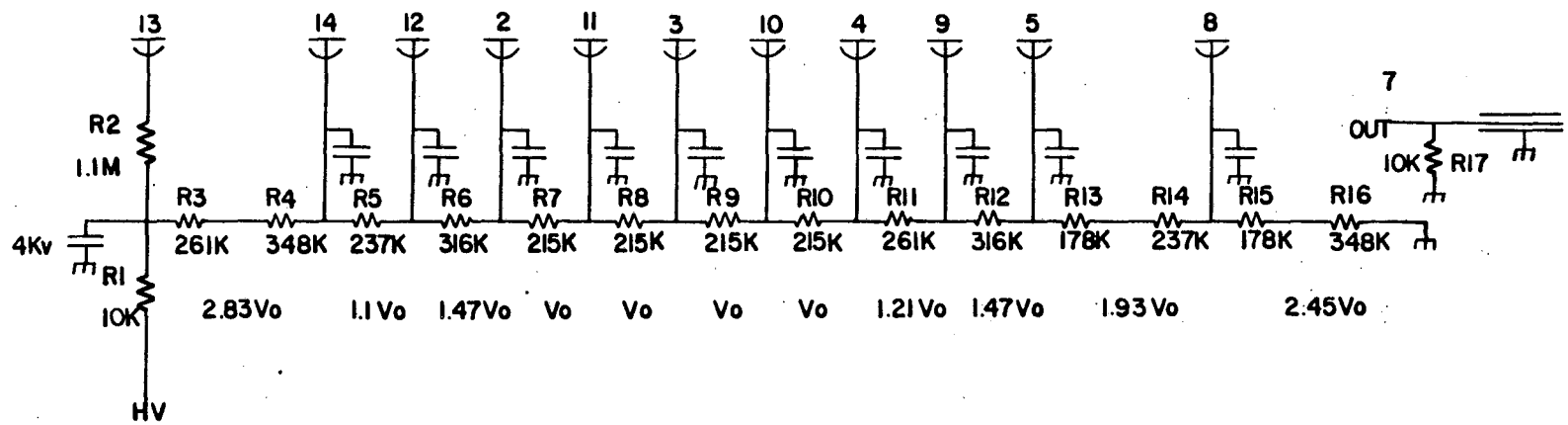

$R_T = 3550\Omega$
Vo = 109 volts
Ro = 215KΩ

Capacitors: 1nf/3Kv

HIGH VOLTAGE DIVIDER FOR XP 2972

FIG. 2

XBL 859-4003

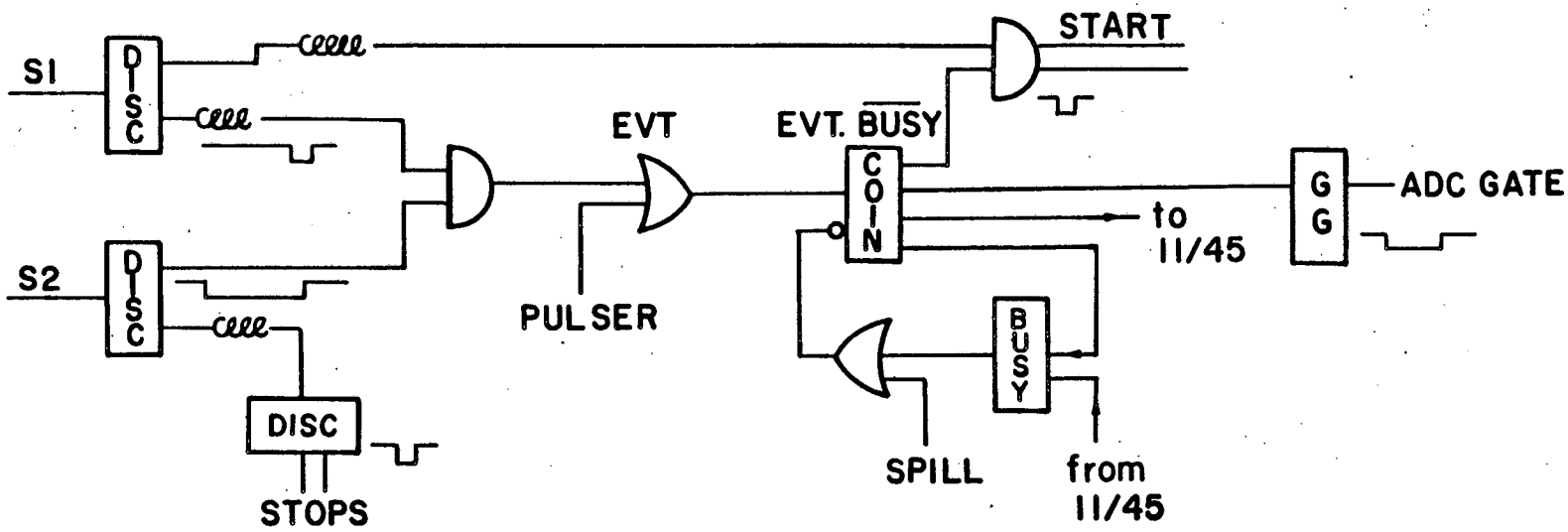

LOGIC FOR TOF MEASUREMENTS

FIG.3

XBL 859-4002

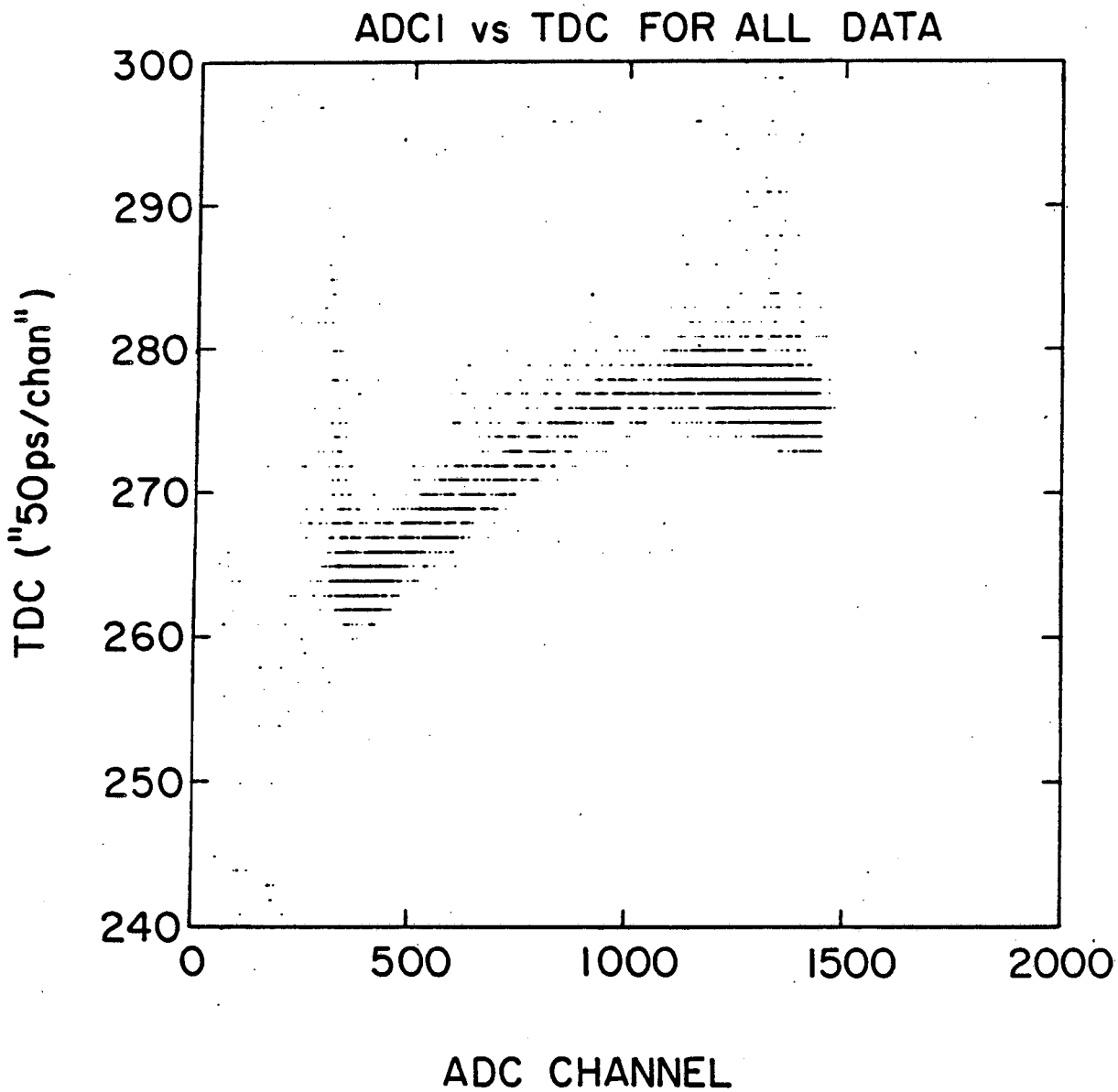

FIG.5

XBL 859-3996

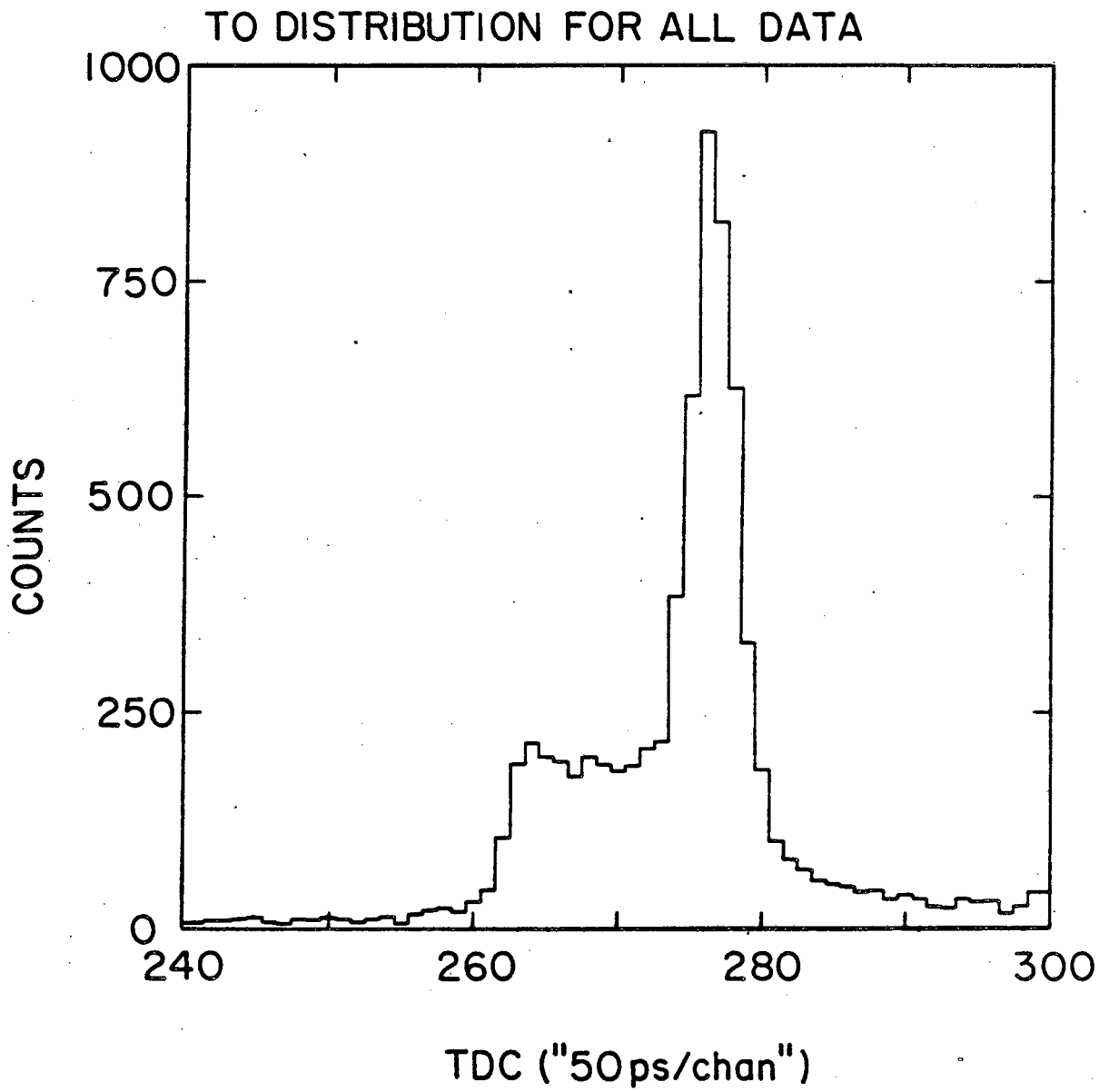

FIG. 4

XBL 859-3998

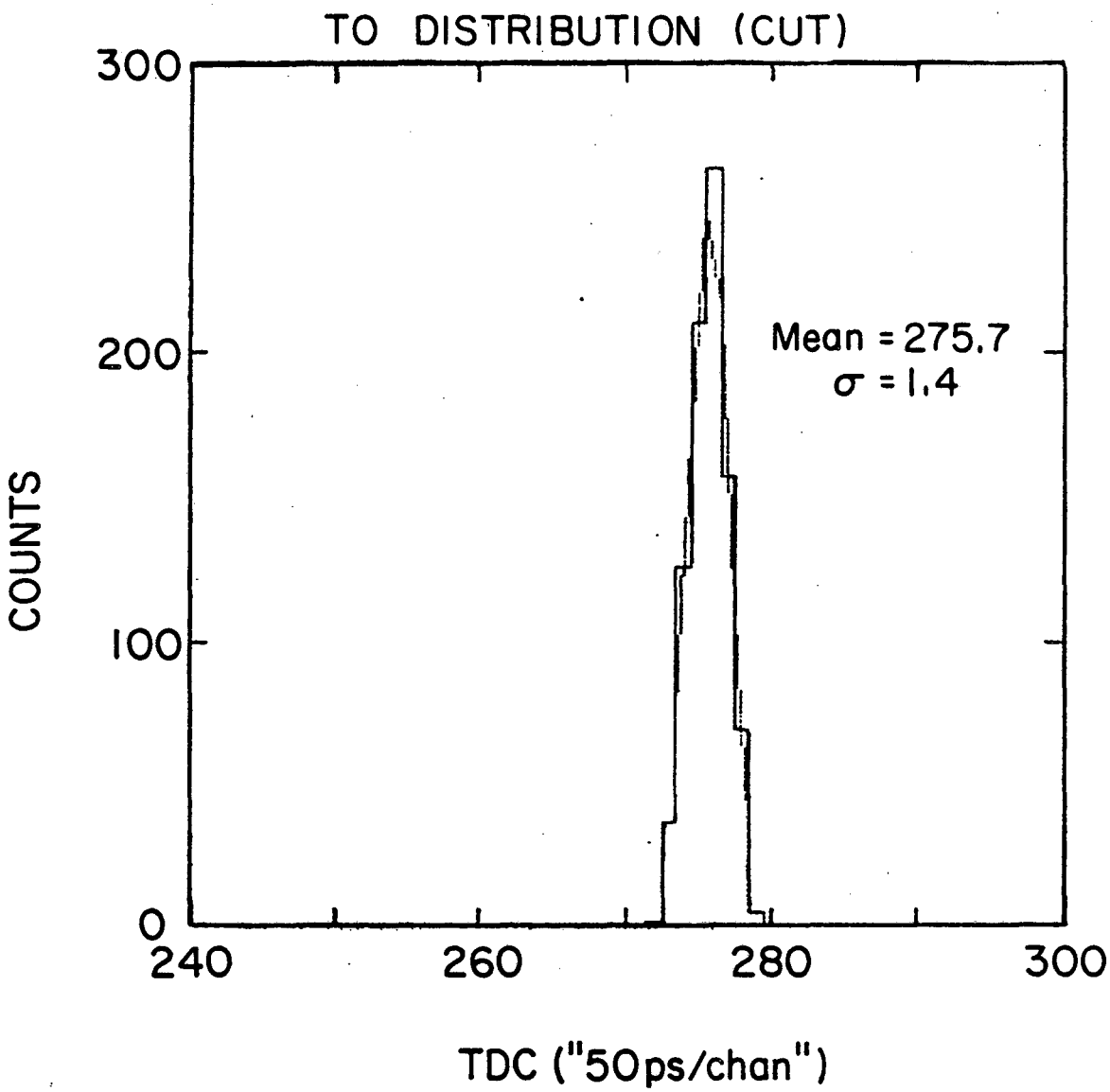

FIG. 6

XBL 859-3997

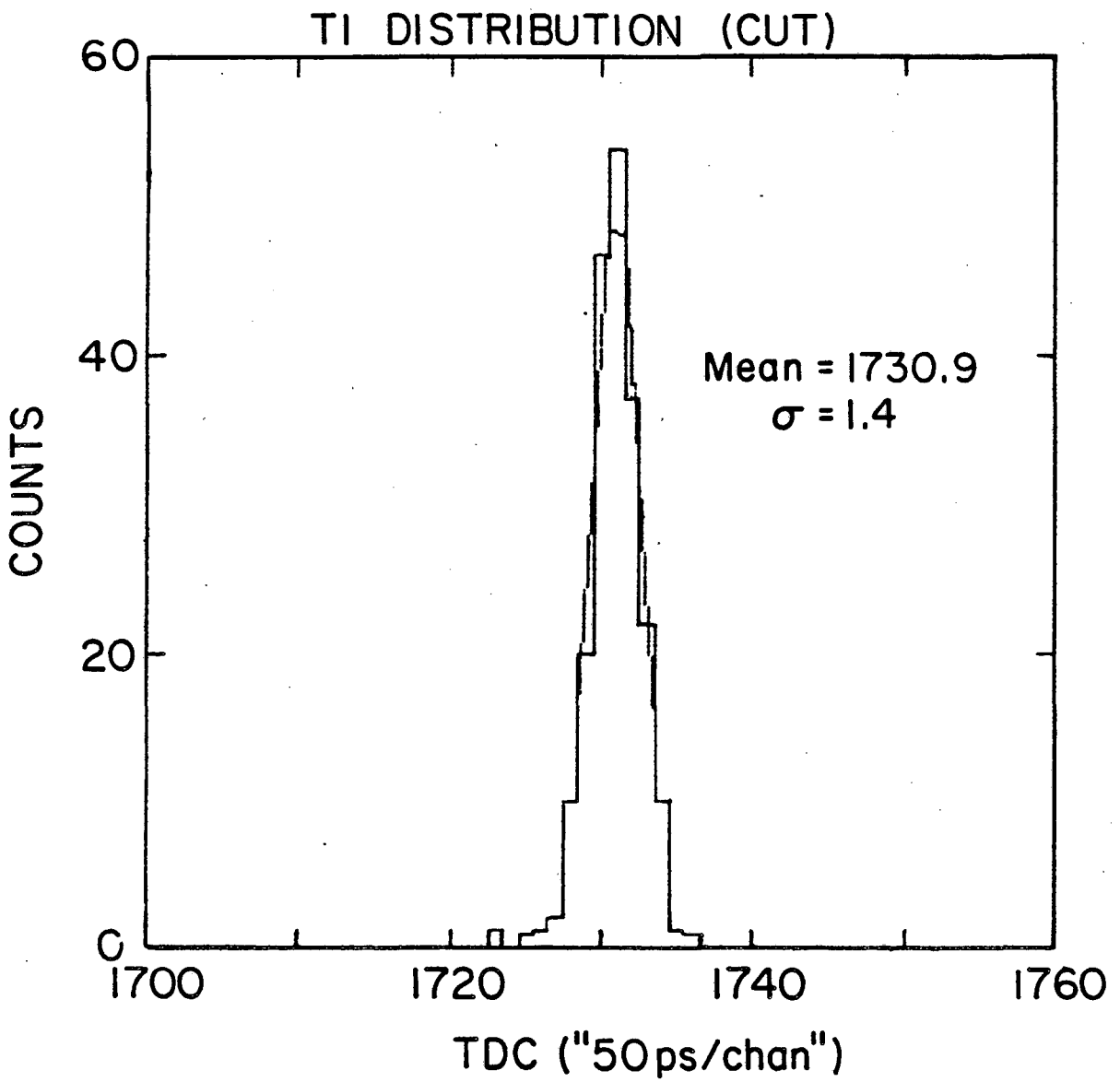

FIG. 7

XBL 859-4001

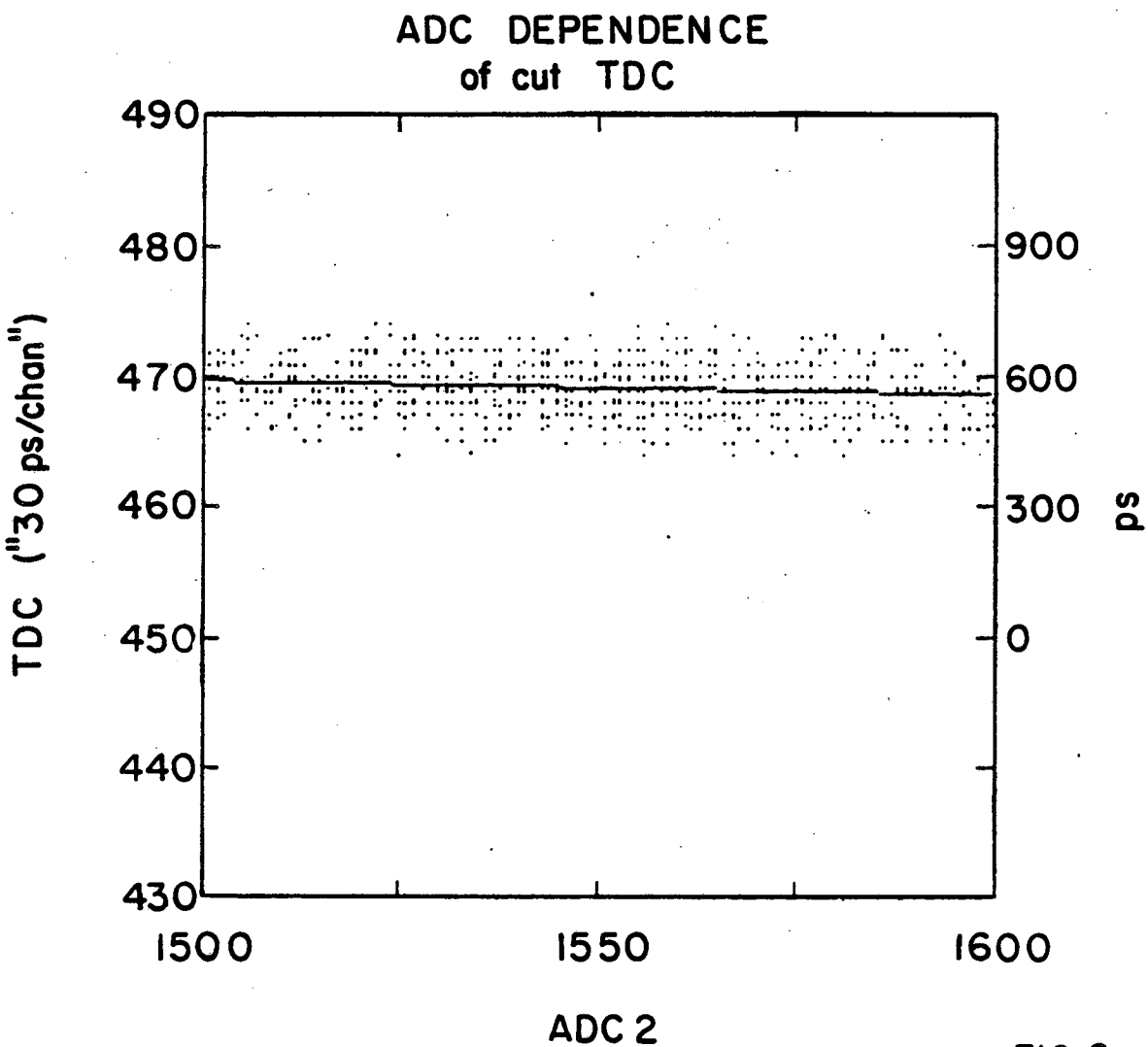

FIG. 8

XBL 859-3999

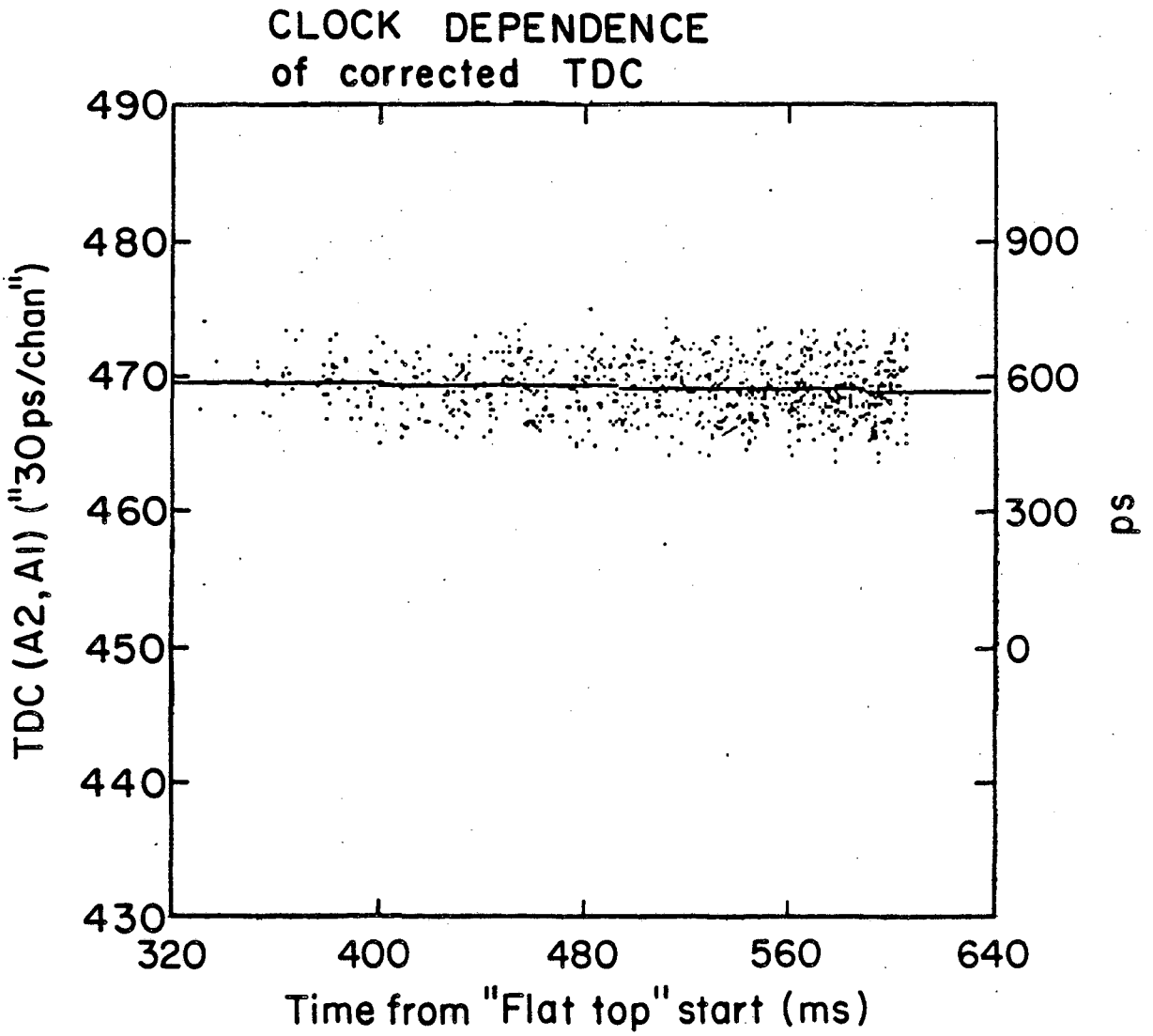

FIG. 9

XBL 859-4000

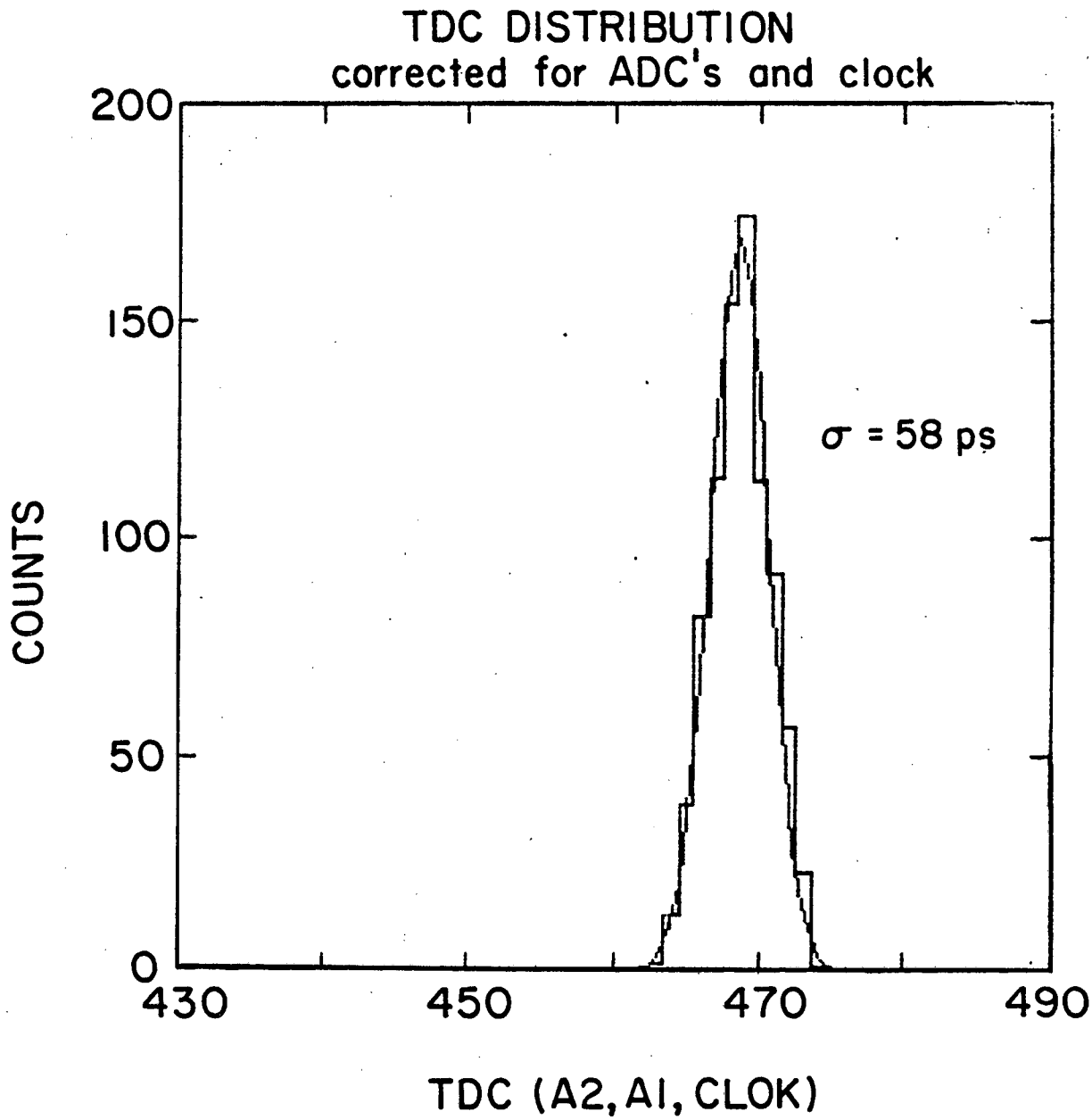

FIG. 10

XBL 859-3995

This report was done with support from the Department of Energy. Any conclusions or opinions expressed in this report represent solely those of the author(s) and not necessarily those of The Regents of the University of California, the Lawrence Berkeley Laboratory or the Department of Energy.

LAWRENCE BERKELEY LABORATORY
TECHNICAL INFORMATION DEPARTMENT
UNIVERSITY OF CALIFORNIA
BERKELEY, CALIFORNIA 94720